

Implementation of strip-area system model for fan-beam collimator SPECT reconstruction

Hongwei Ye¹, Andrzej Krof^{2,1}, David H. Feiglin², Edward D. Lipson^{1,2}, Wei Lee²,
Ioana L. Coman^{3,2}

¹Department of Physics, Syracuse University

²Department of Radiology, SUNY Upstate Medical University

³Department of Mathematics and Computer Science, Ithaca College

ABSTRACT

We have implemented a more accurate physical system representation, a strip-area system model (SASM), for improved fan-beam collimator (FBC) SPECT reconstruction. This approach required implementation of modified ray tracing and attenuation compensation in comparison to a line-length system model (LLSM). We have compared performance of SASM with LLSM using Monte Carlo and analytical simulations of FBC SPECT from a thorax phantom. OSEM reconstruction was performed with OS=3 in a 64×64 matrix with attenuation compensation (assuming uniform attenuation of 0.13 cm⁻¹). Scatter correction and smoothing were not applied. We observe overall improvement in SPECT image bias, visual image quality and an improved hot myocardium contrast for SASM vs. LLSM. In contrast to LLSM, the sensitivity pattern artifacts are not present in the SASM reconstruction. In both reconstruction methods, cross-talk image artifacts (e.g. inverse images of the lungs) can be observed, due to the uniform attenuation map used. SASM applied to fan-beam collimator SPECT results in better image quality and improved hot target contrast, as compared to LLSM, but at the expense of 1.5-fold increase in reconstruction time.

Keywords: strip-area system model, fan-beam collimator SPECT reconstruction, ray tracing, image quality, image artifacts

1. INTRODUCTION

Single photon emission computed tomography (SPECT) is widely used for functional imaging. One of its advantages over positron emission tomography (PET) is SPECT's significantly lower cost. SPECT is extensively applied in nuclear medicine for mapping the regional perfusion of the brain and for myocardial perfusion imaging. This method has been applied to a number of neurological and psychiatric disorders including epilepsy, dementia, and brain trauma; and to myocardial ischemia and viability studies. Since high resolution is crucial in neuroperfusion and myocardial perfusion imaging, ultra-high-resolution parallel-beam collimators (PBCs) and fan-beam collimators (FBCs) have been used to improve system resolution and sensitivity in such studies. FBCs are superior to PBCs because of increased sensitivity. However, the converging beam geometry of FBC may result in truncation artifacts and requires appropriate modification of the reconstruction algorithms that are used for SPECT with PBC. Iterative reconstruction algorithms provide better image quality, compared to filtered back projection (FBP) algorithms, but require ray-driven models of the system transition matrix. The oldest and the most common approach has been a *line-length system model* (LLSM) [1]. This approach suffers from sensitivity artifacts due to unrealistic estimation of the contribution of individual voxels to a given projection. In contrast, a *strip-area system model* (SASM) can provide accurate estimation of the individual voxel contributions to a given projection. SASM has been initially applied for reconstruction in transmission tomography (x-ray CT) in parallel-beam geometry [2]. Here we discuss the implementation of SASM in the ordered-subsets expectation-maximization (OSEM) reconstruction algorithm [3, 4], and apply it to SPECT with FBC phantom studies. The images reconstructed using OSEM with SASM are compared with images reconstructed using OSEM with LLSM by standard evaluation methods including regional analysis, line profiles, accuracy, bias, and contrast.

2. METHOD

2.1. Reconstruction

We have implemented SASM for fan-beam-collimator (FBC) SPECT reconstruction, along with a modified attenuation-compensation approach suitable for SASM. We estimated attenuation of gamma emission from a voxel j directed to a detector unit i using two extreme rays denoted as 1 and 2 in Fig. 1. Two cases have been considered: i) when only one extreme ray traverses voxel j , in which case all activity in this voxel is attenuated as if it was a point source in the middle of the segment of ray 1 or 2 within the voxel, and ii) when two extreme rays traverse voxel j , in which case half the activity in this voxel is attenuated as if it was a point source in the middle of the ray 1 segment within the voxel and the other half as if it was a point source in the middle of the ray 2 segment within the voxel.

Scatter-free and noise-free projections were taken into account in this study (see the next section). The OSEM reconstruction was performed with OS=3 in a 64×64 matrix with attenuation compensation and detector response correction. Scatter correction and smoothing were not applied.

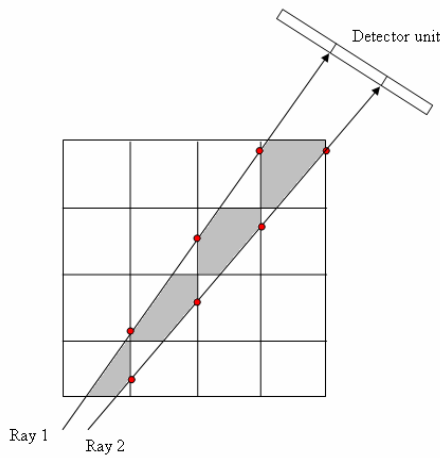


Fig. 1. Strip-area system model. Two extreme rays denoted as 1 and 2 traverse voxels in the reconstruction space. Two extreme rays traverse shaded voxels, while blank voxels are traversed by at most one extreme ray. Two cases were considered: i) when only one extreme ray traverses a voxel, so that all activity in this voxel is attenuated as if it was a point source in the middle of intersection of ray 1 or 2 with the voxel; and ii) when two extreme rays traverse a voxel, so that half of the activity in this voxel is attenuated as if it was a point source in the middle of intersection of the ray 1 with the voxel and the other half as if it was a point source in the middle of intersection of the ray 2 with the voxel.

2.2. Phantom simulations

The Monte Carlo package, SimSET (v2.6.2.5) [5], was used to simulate FBC SPECT Tc-99m data acquired in a 128×64 matrix in 120 views with a circular orbit (focal length equal to 40 cm; radius of rotation equal to 17 cm) and

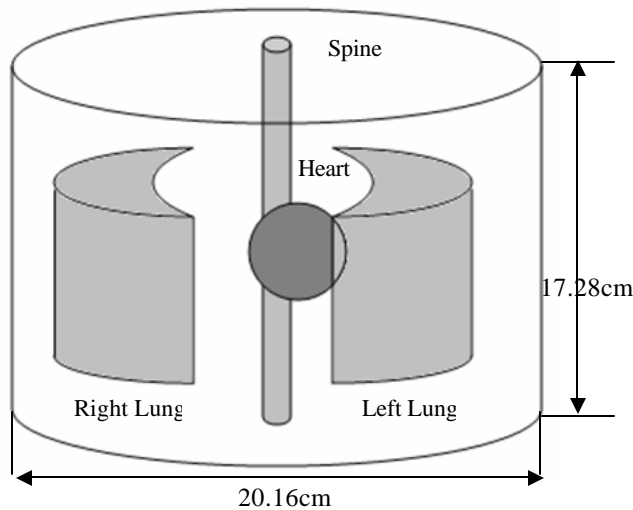


Fig. 2. The digital thorax phantom used for SimSET Monte Carlo Simulations which includes heart, right and left lungs, spine, and other soft tissues (3D front view).

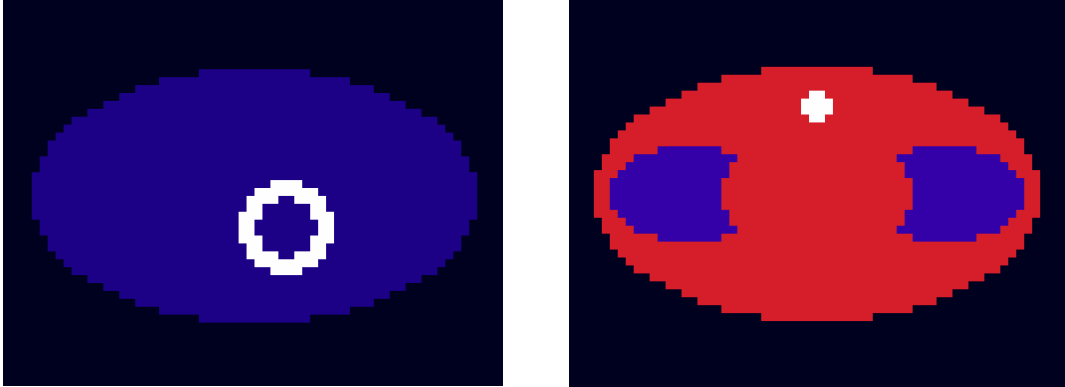


Fig. 3. Emission (left) and attenuation (right) maps of a thorax phantom (slice 35) used for Monte Carlo simulations of fan-beam collimator SPECT with Tc-99m. The myocardium activity is 1.775 $\mu\text{Ci/ml}$. The activity of the remainder of the thorax is 0.1775 $\mu\text{Ci/ml}$. Red: soft tissue ($\mu=0.13 \text{ cm}^{-1}$). Blue: lung tissue ($\mu=0.04 \text{ cm}^{-1}$). White: spine ($\mu=0.30 \text{ cm}^{-1}$).

with an energy window set at 18%. A large number of photon histories (10^9 photons/projection) were simulated to obtain low noise projection data with the scatter estimate.

A thorax phantom was used in this study with a $64 \times 64 \times 64$ matrix and containing Tc-99m activity of 1.775 $\mu\text{Ci/ml}$ in the hot myocardium and 0.1775 $\mu\text{Ci/ml}$ in the remainder of the thorax (Fig. 2). Emission and attenuation maps of this thorax phantom are shown in Fig. 3.

3. RESULTS AND DISCUSSION

The scatter-free projection set was obtained by separately tracking only the primary (scatter-free) photons in the SimSET simulation of Tc-99m SPECT scan with FBC. The first 16 views of scatter-free projection are shown in Fig. 4. These data were reconstructed using OSEM with LLSM and SASM. Figure 5 shows slice 35 of the thorax phantom, and the reconstructed images (20th iteration) using LLSM and SASM. The visual quality of SASM is clearly better than LLSM.

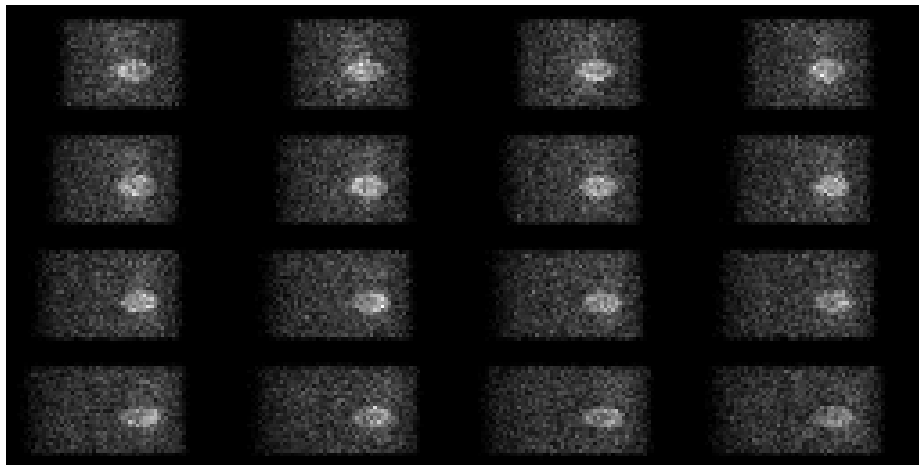


Fig. 4. The first 16 views of scatter-free projection acquired by SimSET simulation of Tc-99m SPECT scan with FBC. Focal length = 40 cm and radius of rotation = 17 cm.

Furthermore, the horizontal and vertical line profiles verify better resolution, and contrast in SASM than in LLSM, as shown in Fig. 6.

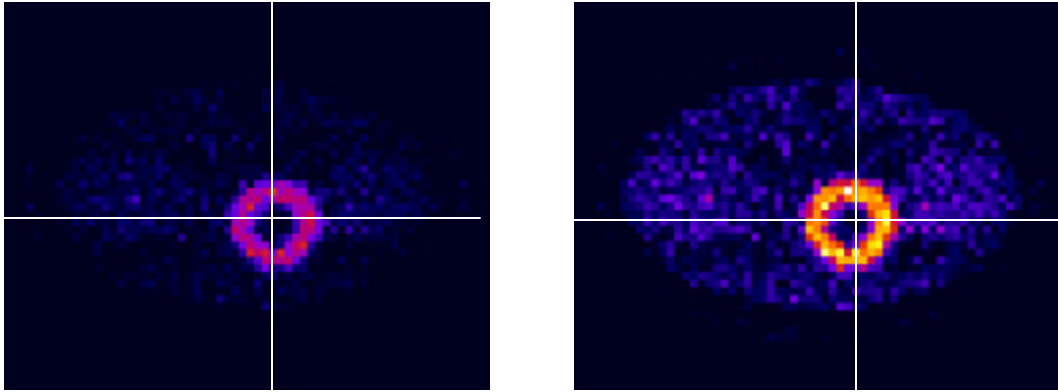


Fig. 5. Slice 35 of reconstructed (OSEM, OS=3; 20 iterations with uniform attenuation) thorax phantom Monte Carlo simulated fan-beam collimator SPECT with Tc-99m. Left: line-length system model (LLSM) reconstruction. Right: strip-area system model (SASM) reconstruction. White lines mark the location of line profiles used in the analysis.

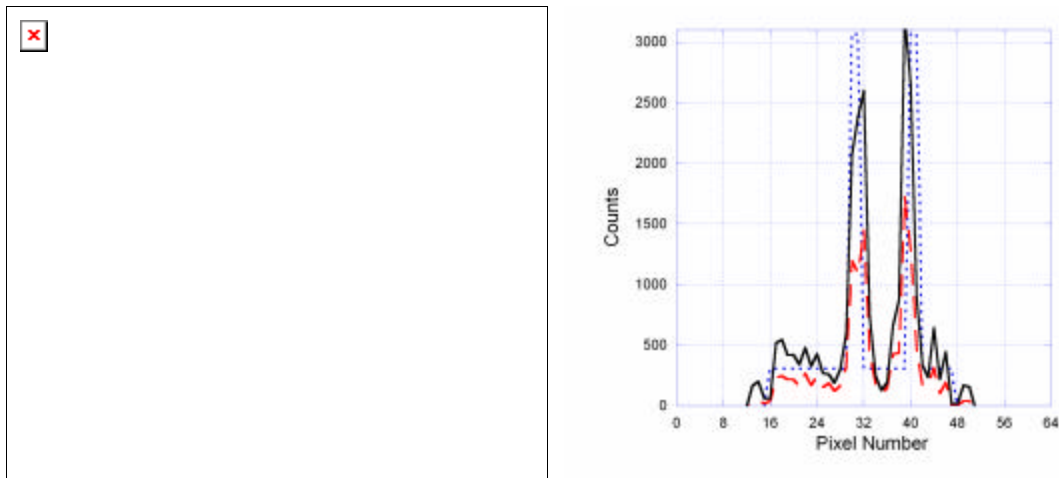


Fig. 6. Horizontal (left) and vertical (right) one-channel-wide line profiles (marked by white lines in Fig. 5) across the reconstructed image of the heart (Monte Carlo fan-beam collimator SPECT simulation, OSEM, OS=3; 20 iterations with uniform attenuation). Blue dotted line: phantom. Red dashed line: LLSM reconstruction. Black solid line: SASM reconstruction.

In addition to visual comparison of images and line profiles, the accuracy and bias were calculated to quantitatively evaluate the two system models. The accuracy was calculated using the normalized mean square error (NMSE) defined by [6]:

$$\% NMSE = 100 \times \left[\frac{\sum_i (x_i - p_i)^2}{\sum_i p_i^2} \right] \quad (1)$$

where i is the pixel index in a region of interest (ROI), x represents the reconstructed image, and p represents the phantom.

The bias was defined by:

$$\%bias = 100 \times \left(\frac{\sum_i x_i - \sum_i p_i}{\sum_i p_i} \right) \quad (2)$$

Four ROIs were chosen to investigate the reconstruction quality of different organs and tissue in the body: right lung, left lung, soft tissue, and myocardium Table 1 shows the %NMSE and %bias values that were obtained. They were calculated for the 20th iteration of both system models. The results indicate that SASM has better accuracy and bias in the thorax phantom, except for the lung regions. The reason for this exception is that the cross-talk image artifacts (inverse images of the lungs) are present in the reconstruction because of the uniform attenuation map used in the reconstruction, instead of the map shown in Fig. 2 The crosstalk between the activity map and the attenuation map is present if no additional attenuation map information is available. Transmission scans [7], segmentation of different body tissues [8, 9] and large penalty in the cost function [10] were reported to suppress this artifact. In order to elucidate the origin of the exception, a true attenuation map was used in the reconstruction, and corresponding %NMSE and %bias values have been obtained (see values in Table 1 after the slashes, “/”). We observe that, in such reconstruction, %NMSE and %bias are better in SASM than in LLSM. This could be explained by the reduction of the crosstalk artifact when a true attenuation map was applied in both system models. Figure 7 gives an example of images reconstructed using OSEM with SASM. The %NMSE and %bias values for the lungs became worse in LLSM when a true attenuation map was applied. Thus LLSM provides a rather poor system model that underestimates or overestimates the contribution of certain voxels to the specific detector bins. On the other hand, SASM yields much smaller %NMSE and %bias values, indicating that this system model is more accurate.

Table 1. %NMSE and %bias for four ROIs and whole phantom in OSEM reconstruction of the simulated fan-beam SPECT from the thorax phantom obtained using LLSM and SASM.

ROI	LLSM		SASM	
	%NMSE	%bias	%NMSE	%bias
Whole phantom	38.6	-47.6	31.2	1.3
Right lung*	13.9 / 24.4	-18.9 / -44.1	67.8 / 22.7	54.9 / 0.83
Left lung*	13.3 / 24.7	-15.6 / -44.9	72.4 / 21.3	58.2 / 0.17
Soft tissue	27.8	-43.4	26.0	-9.6
Myocardium	35.5	-58.6	9.2	-20.4

* Values are provided with uniform attenuation map / exact attenuation map for right and left lungs.

The average contrast between myocardium (hot target) and soft tissue (cold target) vs. iteration number for LLSM and SASM is shown in Fig. 8. We observe better average contrast for images reconstructed using OSEM with SASM, as compared to OSEM with LLSM. As expected, the average contrast increases with iteration number in both system models.

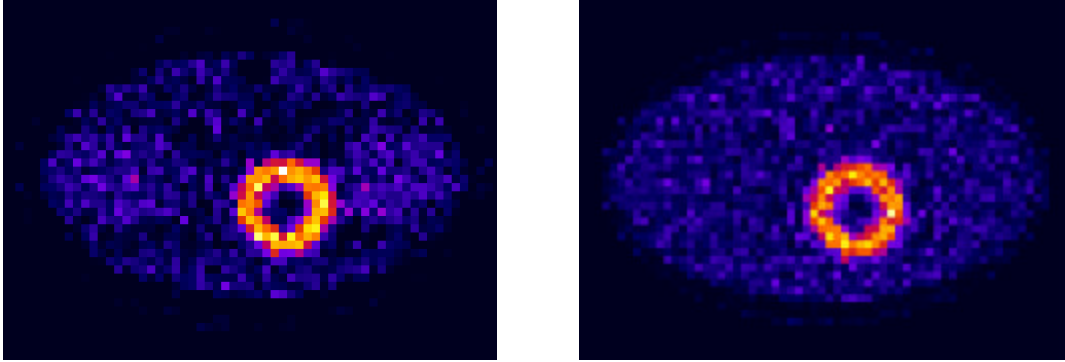


Fig. 7. Slice 35 of reconstructed (OSEM with strip-area system model, OS=3; 20 iterations) thorax phantom Monte Carlo simulated fan-beam collimator SPECT with Tc-99m. Left: with uniform attenuation map. Right: with true attenuation map. Note that the crosstalk artifact (inverse image of the lungs; see Fig. 3 right panel) is not visible in the right image.



Fig. 8. Average contrast defined as $(\text{target} - \text{background}) / (\text{target} + \text{background})$ vs. iteration number for LLSM and SASM. Blue dotted line: phantom. Red dashed line and red standard error bars with circles: LLSM reconstruction. Black solid line and black standard errors with squares: SASM reconstruction. Where target represents the myocardium.

4. CONCLUSIONS

Based on the thorax phantom studies, we conclude that OSEM with SASM applied to fan-beam-collimator SPECT yields better image quality, lower bias, and improved myocardium/soft tissue contrast, as compared to OSEM with LLSM, but at the expense of increased reconstruction time (almost 1.5-fold). Further studies are planned with more advanced phantoms such as NCAT [11], and including scatter and attenuation correction.

OSEM with SASM reconstruction offers a promising tool for improved reconstruction of the SPECT studies with a fan-beam collimator. However, more work is needed to accelerate the reconstruction and to investigate diagnostic performance of this method, before it can be clinically implemented for mapping the regional perfusion of the brain and for myocardial perfusion imaging.

REFERENCES

- [1] Robert L. Siddon, "Fast calculation of the exact radiological path for a three-dimensional CT array", *Med. Phys.*, 12(2), pp. 252-255, 1984
- [2] Shin-Chung B. Lo, "Strip and line path integrals with a square pixel matrix: a unified theory for computational CT projections", *IEEE Trans. Med. Imaging*, 7(4), pp. 355-363, 1988
- [3] K. Lange and R. Carson, "EM reconstruction algorithms for emission and transmission tomography", *J. Comput. Assist. Tomogr.*, 8(2), pp. 306-316, 1984
- [4] H. M. Hudson, R. S. Larkin, "Accelerated image reconstructing using ordered subsets of projection data", *IEEE Trans. Med. Imaging*, 13, pp. 601-609, 1994
- [5] R. L. Harrison, D. R. Haynor, S. B. Gillispie, S. D. Vannoy, M. S. Kaplan, and T. K. Lewellen, "A public-domain simulation system for emission tomography: photon tracking through heterogeneous attenuation using importance sampling", *J. Nucl. Med.*, 34, pp. 60P, 1993
- [6] Y. K. Dewaraja, M. Ljungberg, and J. A. Fessler, "3-D Monte Carlo-based scatter compensation in quantitative I-131 SPECT reconstruction", preprint, www.eecs.umich.edu/~fessler/papers/files/preprint/yuni,tns.pdf, 2005
- [7] A. Krol, J. E. Bowsher, S. H. Manglos, D. H. Feiglin, M. P. Tornai, F. D. Thomas, "An EM algorithm for estimating SPECT emission and transmission parameters from emission data only", *IEEE Trans. Med. Imaging*, 20(3), pp. 218-232, 2001
- [8] J.W.Wallis, T. R. Miller, and P. Koppel, "Attenuation correction in cardiac SPECT without a transmission measurements," *J. Nucl. Med.*, 36, pp. 506 - 512, 1995
- [9] T.-S. Pan, M. A. King, D. J. de Vries, and M. Ljungberg, "Segmentation of the body and lungs from scatter and photopeak window data in SPECT: A Monte Carlo investigation," *IEEE Trans. Med. Imag.*, 15, pp. 13-24; 394-396, 1996.
- [10] Andrei V. Bronnikov, "Reconstruction of attenuation map using discrete consistency conditions", *IEEE Trans. Med. Imaging*, 19(5), pp. 451- 462, 2000
- [11] W. P. Segars and B. M. W. Tsui, "Study of the efficacy of respiratory gating in myocardial SPECT using the new 4D NCAT Phantom", *IEEE Trans. Nucl. Sci.*, 49(3): pp. 675-679, 2002